J Mater Sci (2009) 44:4763–4775
DOI 10.1007/s10853-009-3668-4

REVIEW

Dependence of luminescence properties on composition of rare-earth activated (oxy)nitrides phosphors for white-LEDs applications

Xiang-Hong He · Ning Lian · Jian-Hua Sun · Ming-Yun Guan

Received: 10 April 2009 / Accepted: 5 June 2009 / Published online: 18 June 2009

Abstract Rare-earth-activated nitride and oxynitride phosphors are attractive converter materials for white-LEDs applications due to their efficient luminescent characteristics, high thermal and chemical stabilities because their basic crystal structure is built on rigid tetrahedral networks, either of the Si–(O,N) or Al–(O,N) type. Recent progress in fluorescence properties of silicon–aluminum–(oxy)nitride-based luminescent materials with broad excitation bands activated by Eu^{2+}, Ce^{3+}, and Yb^{2+} for phosphor-converted white-LEDs are reviewed in this article, with the emphasis on the dependence of luminescence properties on composition. We elaborate on these composition-dependent properties in three sections: (i) Eu^{2+}-activated nitride and oxynitride phosphors; (ii) Ce^{3+}-activated nitride and oxynitride phosphors; and (iii) Yb^{2+}-doped α-SiAlON phosphor. Eu^{2+}- or Ce^{3+}-activated nitride and oxynitride phosphors are categorized into four parts following the structural and/or composition characteristics, i.e., α-SiAlON, β-SiAlON, oxonitridosilicates, nitridoalumosilicates, and nitridosilicates. Some involving aspects for designing and the trends of research and development of these phosphors are addressed at the end of this article.

X.-H. He (✉) · N. Lian · J.-H. Sun · M.-Y. Guan
School of Chemistry and Chemical Engineering, Jiangsu Teachers University of Technology, Changzhou, Jiangsu 213001, People's Republic of China
e-mail: hexh@jstu.edu.cn

X.-H. He · N. Lian · J.-H. Sun · M.-Y. Guan
Jiangsu Province Key Laboratory of Precious Metal Chemistry and Technology, Changzhou, Jiangsu 213001, People's Republic of China

Introduction

Due to its energy savings, positive environment effects, and most challenging application as a replacement for conventional incandescent bulbs and fluorescent lamps, more and more interest has been focused on the phosphor-converted white light-emitting diodes (pc-white-LEDs) made of UV or blue emitting chips coated by phosphors, as a novel generation of solid-state lighting (SSL) devices [1–7]. In pc-white-LEDs, GaN or InGaN semiconductor chips which emit near-UV light of 370–410 nm or blue light of 450–470 nm are adopted as a primary light source. Therefore, it is necessary and preferable for conversion phosphors to have a wide excitation band covering these wavelength ranges. Luminescence conversion of near-UV or blue light into longer wavelength radiation applied in state-of-the-art white LEDs poses new challenges in phosphor research, especially, in view of the small energy difference between pump and emission wavelength. The search for new phosphors which can convert the near-UV or blue emission from (In,Ga)N LEDs chips into visible light, is becoming a worldwide scientific concern in the field of luminescent materials [8–10]. In the search for new inorganic phosphors used in pc-white-LEDs, luminescent materials with high efficiency, stability, no environmental hazards, and high charge densities between activator and its surroundings are expected.

Some well-known rare-earth (RE) activator ions, such as Eu^{2+}, Ce^{3+}, Yb^{2+}, etc., exhibit broadband absorption and emission characteristic from 5d → 4f transition [4, 11]. Thus, they are suitable activators for phosphors used in pc-white-LEDs. The crystal field environment and nephelauxetic effect in different host lattices make the emission spectra of Eu^{2+}, Ce^{3+}, or Yb^{2+}-doped phosphor vary from ultraviolet to red region, which is of great importance for

phosphor design and practical applications. To the large extent, the luminous efficiency of phosphor depends on the matrix. Host lattices with a high degree of covalency and/or a large crystal field splitting at the site for which Ce^{3+} or Eu^{2+} substitute can lead to efficient visible emission while absorbing the near-UV to blue light. All possible variations in host composition may alter the symmetry, covalence, crystal field strength, and the energy transfer, thus influencing the luminous efficiency and property. To tune the optical properties of these activator ions as to their suitability in pc-white-LEDs, apart from well-known yttrium–aluminum–garnet YAG:Ce^{3+} [3, 12–14], many new nitrides and oxynitrides based on $[(Si,Al)(O,N)_4]$ tetrahedral building units have been recently developed because of the higher formal charge of N^{3-} compared with O^{2-} and the stronger nephelauxetic effect than that in an analogous oxygen environment. Due to their excellent properties, such as non-toxicity, outstanding thermal and chemical stability, broad available range of excitation and emission wavelengths, and high luminescence efficiency upon activation using RE ions, the novel class of (oxy)nitride phosphors has demonstrated its superior suitability for use in white LEDs.

Several reviews have been published on nitride and oxynitride phosphors for pc-white-LEDs in recent years [15–17]. However, these reviews are either too focused on the preparation and crystal structure, or rather luminescent properties and application characteristics. With an exact knowledge of the dependence of luminescence on the crystal structure and composition of the host lattice, it would be feasible to design luminescent materials with desired properties. This Review article is intended to provide an overview of component design and fluorescence properties of RE-activated nitride and oxynitride phosphors for white LEDs applications. The dependence of spectroscopic properties on composition was summarized. In the main context, Eu^{2+}- or Ce^{3+}-activated nitride and oxynitride phosphors are categorized into four parts following the structural and/or composition characteristics, i.e., α-SiAlON, β-SiAlON, oxonitridosilicates, nitridoalumosilicates, and nitridosilicates. Then, the luminescence properties of Yb^{2+}-activated α-SiAlON phosphor were briefly reviewed. Finally, issues on design of efficient nitride and oxynitride-based phosphors for pc-white-LEDs were considered.

Eu^{2+}-activated nitride and oxynitride phosphors

Divalent europium ion (Eu^{2+}) is one of the important activators for luminescent materials. The emission and absorption spectra of Eu^{2+} usually exhibit broadbands due to transitions between the $^8S_{7/2}$ ($4f^7$) ground state and the $4f^6$5d excited state. Depending on the type of host lattice in terms of site size, site symmetry, and coordination number, Eu^{2+} luminescence varies from ultraviolet to red, which is mainly influenced by the covalency and strength of the crystal field [11]. Due to the higher formal charge and greater covalent character of N^{3-} than O^{2-}, the incorporation of Eu^{2+} in nitrogen-containing crystal lattices can lead to very interesting luminescence properties which are significantly different from those that can be found in oxide environments. In this section, we will review the dependence of spectroscopic properties on composition of Eu^{2+}-activated nitrides and oxynitrides.

Eu^{2+}-activated α-SiAlON

α-SiAlONs, isostructural with α-Si_3N_4, are solid solutions of the M–Si–Al–O–N system, which have a structure derived from α-Si_3N_4 with the general formula $M_x^{v+}Si_{12-(m+n)}Al_{m+n}O_nN_{16-n}$, where $x = m/v$, v is the valency of modifying cation M, and M is one of the cations Li, Mg, Ca, Y, and some RE [18–20]. The studies on the absorption spectra of RE-doped α-SiAlON ceramics [21, 22], open the door for α-SiAlON ceramics used as phosphors. The findings of longer wavelength luminescence in RE-doped α-SiAlON enable α-SiAlON to be used in white-LEDs devices. By controlling the overall composition of the α-SiAlON host lattice or by altering the Eu^{2+} doping concentration, the photoluminescence properties can be tailored. Therefore, RE-activated α-SiAlON luminescence materials, especially Eu^{2+}-activated α-SiAlON, are attracting much attention in recent years [23–30].

In comparison with other α-SiAlONs, Ca–α-SiAlON can accommodate the largest concentration of the modifying cations, and even the largest La^{3+} cation [31]. Meanwhile, the $\alpha \rightarrow \beta$ reverse phase transformation that usually occurs during annealing of α-SiAlONs at intermediate temperatures [32–34], has not been observed in Ca–α-SiAlON [35], suggesting the good thermal stability of Ca–α-SiAlON. Eu^{2+}-doped Ca–α-SiAlON shows a board band emission peaking at yellow and orange region [23, 24, 26]. According to Xie and coworkers [23–25], the luminescence properties of Eu^{2+}-doped Ca–α-SiAlON with the normal compositions $(Ca_xEu_y)Si_{12-(m+n)}Al_{(m+n)}O_nN_{16-n}$ ($x = 0.2$–2.2, $y = 0$–0.25) yellow phosphors, depend greatly on the Eu^{2+} concentration and the overall composition of the host lattice. As shown in Fig. 1, two broadbands are observed in the excitation spectrum with maxima at ~300 and 400 nm, respectively. The emission spectra of these phosphors show a single intense broad emission band at 583–603 nm. The emission band systematically red-shifts as the Eu^{2+} concentration or the Ca^{2+} content increases, which is due to less rigidity of lattice and the splitting of 5d electrons of Eu^{2+} caused by changes in crystal field (Figs. 1, 2).

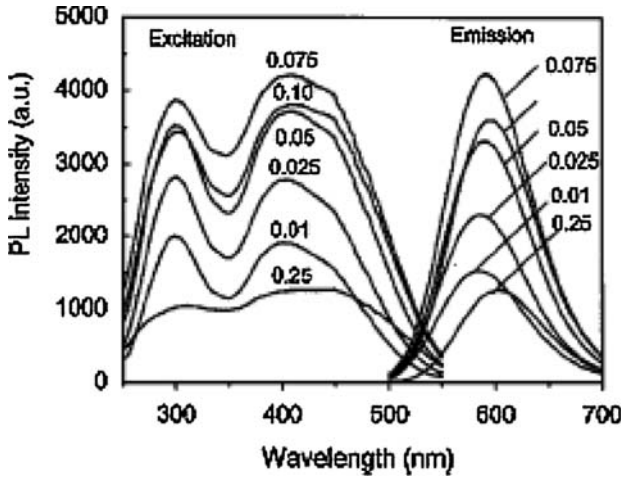

Fig. 1 Excitation (*left*, monitoring wavelength $\lambda_{em} = 590$ nm) and emission (*right*, excitation wavelength $\lambda_{ex} = 450$ nm) spectra of Ca–α-SiAlON:yEu^{2+} with different Eu concentration ($0.01 \leq y \leq 0.25$) [23]

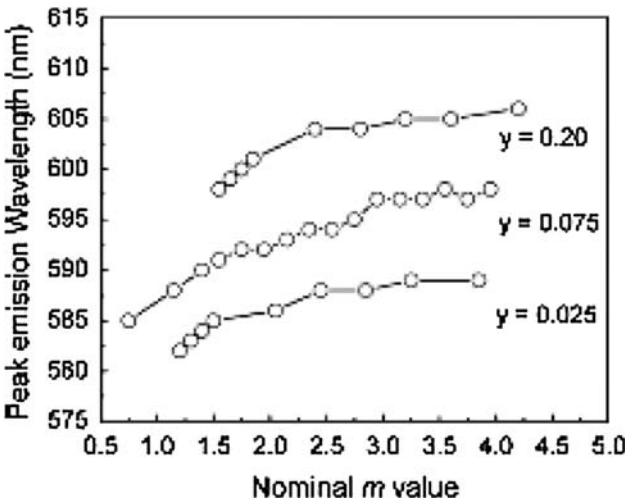

Fig. 2 Graph of peak emission wavelength vs. the overall composition m of $(Ca_xEu_y)Si_{12-(m+n)}Al_{(m+n)}O_nN_{16-n}$ for different Eu concentration ($m = 2x + 2y$) [24]

Similar to Ca–α-SiAlON:Eu^{2+}, the excitation spectrum of Li–α-SiAlON:Eu^{2+} comprises two dominant peaks at ~300 and 435–449 nm, respectively [29, 30]. However, the intensity at 435–449 nm is more intense than that at ~300 nm in comparison with Ca–α-SiAlON:Eu^{2+}. This indicates that Li–α-SiAlON:Eu^{2+} absorbs more strongly in the blue light region, which matches well with the emission of blue LEDs chips. The emission wavelength of Li–α-SiAlON:Eu^{2+} phosphors with compositions of $(Li_{1-2y}Eu_y)_mSi_{12-m-n}Al_{m+n}O_nN_{16-n}$ ($0.5 \leq m \leq 2.0$, $0.5 \leq n \leq 2.0$, and $0.5 \leq y \leq 18$ mol.%), can be tuned in a wide range of 563–586 nm by tailoring the Al/Si or O/N ratios of the host lattice or by controlling Eu^{2+} concentration [29]. These phosphors emit greenish-yellow light under the blue excitation, about 15–35 nm shorter than the Ca–α-SiAlON:Eu^{2+} phosphor, allowing it to create cool white light when coupled to a blue LEDs chip. Li–α-SiAlON:Eu^{2+} has a smaller Stokes shift (4,900–5,500 cm^{-1}) than Ca–α-SiAlON:Eu^{2+} (7,000–8,000 cm^{-1}). The absorption and external quantum efficiencies of this phosphor can reach 70 and 40% under the 460 nm excitation, respectively. White LEDs using Li–α-SiAlON:Eu^{2+} and InGaN-based blue LED chip, owns promising optical properties: correlated color temperature CCT = 6,150 K, luminous efficiency $\eta_L = 43$–55 lm/W, and color rendering index $R_a = 60$–72. Compared to white LEDs made with Ca–α-SiAlON:Eu^{2+}, the white LEDs fabricated with Li–α-SiAlON:Eu^{2+} exhibited higher CCT values and higher CRI values. Therefore, highly efficient daylight emission, which is not achieved in white LEDs fabricated with the Ca–α-SiAlON:Eu^{2+}, can be generated using Li–α-SiAlON:Eu^{2+} [30].

For (Ca,Y)–α-SiAlON:Eu^{2+} phosphors with nominal compositions of $(Ca_{1-p}Y_p)_{0.88}$ $Si_{12-(m+n)}Al_{m+n}O_nN_{16-n}$: 0.05Eu^{2+}, a red shift of emission wavelength occurred when Ca was partially replaced by Y [27, 28]. The peak emission wavelength varied from 585 to 601 nm, with increasing of the Y content, and therefore the chromaticity range of (Ca,Y)–α-SiAlON phosphors extended to longer wavelength [28].

In one word, with aiming to design M–α-SiAlON:Eu^{2+} phosphors with desired excitation and luminescent wavelength, the following factors should be considered: proper choice modifying cation M, tailoring the Al/Si or O/N ratios, or controlling the Eu^{2+} concentration.

Eu^{2+}-doped β-SiAlON

β-SiAlON is derived from β-Si_3N_4 by equivalent substitution of Al–O for Si–N, and its chemical composition can be written as $Si_{6-z}Al_zO_zN_{8-z}$ (z represents the number of Al–O pairs substituting for Si–N pairs and $0 < z \leq 4.2$) [36–40]. So far, compared to α-SiAlON-based phosphors, the studies of RE-doped β-SiAlON luminescence materials are very limited [41–44]. Here, we take Eu^{2+}-activated β-SiAlON as an example, for implying the relationship between the luminescent properties and compositions of β-SiAlON-based phosphors.

Eu^{2+}-activated β-SiAlON green-emitting phosphor was recently invented by the group of Hirosaki [41]. Thereafter, the studies revealed that β-SiAlON:Eu^{2+} has a small thermal quenching and high stability of chromaticity against temperature [42]. It can be excited efficiently over a broad spectral range between 280 and 480 nm and exhibits an intense green emission peaked at 528–550 nm. The internal quantum efficiency of the β-SiAlON:Eu^{2+} phosphor is 54%, and 50% at the excitation wavelength of 405 and 450 nm,

respectively, and the corresponding external quantum efficiency is 41%, and 33%. It has a superior color chromaticity of (0.32,0.64). Compared to ZnS:Cu,Al and $Y_3Al_5O_{12}:Ce^{3+}$ green-emitting phosphors, the β-SiAlON:Eu^{2+} phosphor has better color saturation and thermal stability. Thus, a white LED with an ultrahigh color rendering index ($R_a > 95$) by utilizing this β-SiAlON:Eu^{2+} phosphor in combination with other oxynitride phosphors and a blue LED chip was successfully prepared [43].

As for $Si_{6-z}Al_zO_zN_{8-z}:Eu^{2+}$, with the z values changing in the range of 0.25–2.0, its photoluminescence intensity and peak differed [44]. As z values increased, emission intensities decreased and the emission bands shifted towards longer wavelength side (Fig. 3). The emission peaks of the phosphors having z values of 0.5, 1.0, and 2.0 were located at 540, 545, and 548 nm, respectively. The phenomenon of red shift of emission peak can be attributed to the Stokes shift effect caused by the decreased rigidity of the β-SiAlON with larger z values. It is clear that Eu^{2+}-doped β-SiAlON having small z values ($z < 1.0$) is considered to be useful phosphor materials due to its high-luminescence strength.

Eu^{2+}-activated oxonitridosilicates

The group of van Krevel pioneered the synthesis of oxonitridosilicate-based luminescent materials [45]. Thereafter, the photoluminescence properties of Eu^{2+}-activated oxonitridosilicates phosphors such as $MSi_2O_{2-\delta}N_{2+2/3\delta}:Eu^{2+}$ (M = Ca, Sr, Ba) [46], $MSi_2O_2N_2:Eu^{2+}$ (M = Ca, Sr, Ba) [47–52], and $BaAl_{2-x}Si_xO_{4-x}N_x:Eu^{2+}$ [53, 54] were reported. Here, we will summarize the relationship between the composition and luminescence of these phosphors. In addition, two reported examples of Eu^{2+}-activated oxonitridosilicates phosphors with shorter wavelength emission are given.

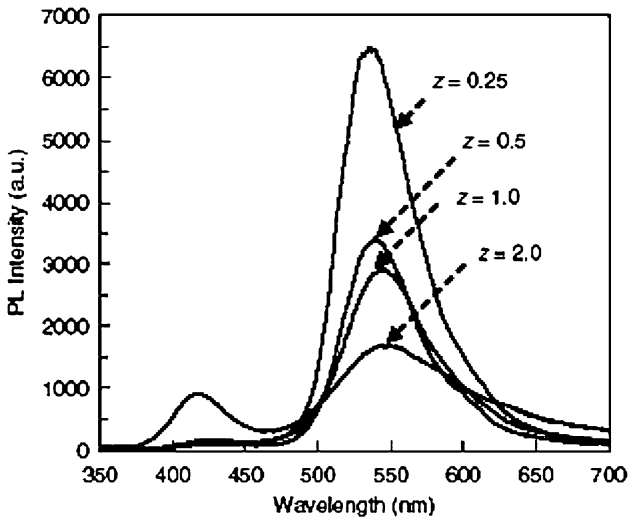

Fig. 3 Emission spectra of Eu^{2+}-doped β-SiAlON ($Si_{6-z}Al_zO_zN_{8-z}:Eu^{2+}$) phosphors with varying z values ($\lambda_{ex} = 303$ nm) [44]

Li and coworkers reported on the composition-dependent luminescence properties of $MSi_2O_{2-\delta}N_{2+2/3\delta}:Eu^{2+}$ (M = Ca, Sr, Ba) phosphors [46]. These phosphor show a typical broadband emission and can be efficiently excited in the blue region of the spectrum, which perfectly matches with the radiation of the blue-InGaN chips. The position of the emission band differs with the type of M ions. However, the peak of excitation bands of $MSi_2O_{2-\delta}N_{2+2/3\delta}:Eu^{2+}$ materials is very similar for M = Ca, Sr, Ba. Excitation into the UV–blue range (370–450 nm), Eu^{2+}-doped $MSi_2O_{2-\delta}N_{2+2/3\delta}$ (M = Ca, Sr, Ba) exhibits efficient blue-green emission at 490–500 nm for M = Ba, whereas yellow and green-yellowish emission at 560 and 530–570 nm were found for M = Ca and M = Sr, respectively [46].

The Schnick's group systematically presented the detailed structure investigation of $MSi_2O_2N_2$ (M = Ca, Sr, Ba) and $EuSi_2O_2N_2$ [55–58]. It is found that $CaSi_2O_2N_2$ and $SrSi_2O_2N_2$ show similar crystal structure but not isotypic. As expected, the M in $CaSi_2O_2N_2$ and $SrSi_2O_2N_2$ can undergo ion exchange and then form solid solution. Recently, $MSi_2O_2N_2$ (M = Ca, Sr, Ba) was identified as a promising new class of host lattices for divalent RE-doped phosphors [47–52]. The emission color tuning of $Sr_{1-x-y-z}Ca_xBa_ySi_2O_2N_2:zEu^{2+}$ phosphors are investigated by Yun et al. [47], Zhang et al. [50], and Bachmann et al. separately [51]. An intense yellowish-green to greenish-yellow tunable emission can be obtained by changing the mole ratio of Sr/Ca of $(Ca_{1-x-y}Sr_x)Si_2O_2N_2:yEu^{2+}$. With an increase in x values, the excitation and emission spectra show a red shit and blue shift, respectively [50]. Similarly, after partial substitution of Sr in $Sr_2Si_5N_8:Eu^{2+}$ by Ba, the emission peak of $(Sr_{1-u}Ba_u)Si_2O_2N_2:Eu^{2+}$ shifted from green to yellow through varying Ba fraction u [47, 51]. The substitution of the host lattice cation by other isovalent cation is therefore the most suitable way to tune emission color of oxonitridosilicate phosphors for pc-white-LEDs. Furthermore, the luminescence intensity of $SrSi_2O_2N_2:Eu^{2+}$ can be remarkably enhanced by codoping with Ce^{3+}, Dy^{3+}, and Mn^{2+} [52].

Eu^{2+}-doped MAl_2O_4 (M = Ca, Sr, Ba) were widely used as persistent luminescent materials [53]. Their excitation bands do not match the UV–blue emission (370–460 nm) from InGaN LEDs chips. And modification of the framework of Al_mO_n-containing compounds by replacement of $(AlO)^+$ by $(SiN)^+$ can modify its luminescence to suit white light LED applications [12, 59–62]. Li and coworkers studied the modification of the luminescence properties of $BaAl_{2-x}Si_xO_{4-x}N_x:Eu^{2+}$ by adjusting the amount of $(SiN)^+$ (Fig. 4) [54]. It is found that the maximum solubility of $(SiN)^+$ in $BaAl_2O_4$ lattice is about $x \approx 0.6$ (i.e., 30 mol.%). With the content of incorporated $(SiN)^+$ increasing, an additional

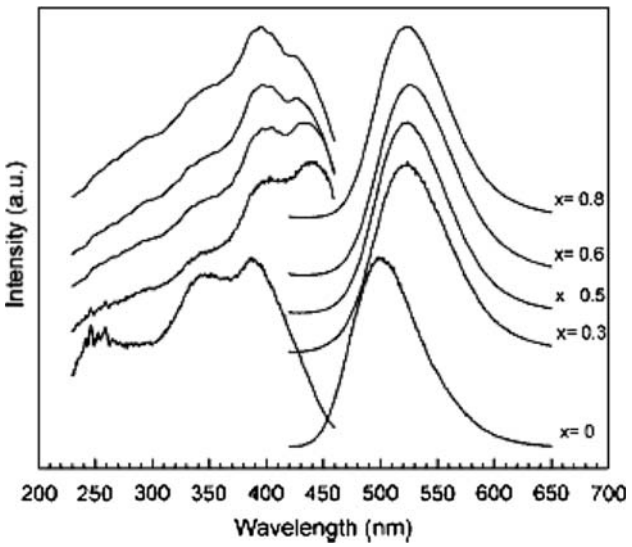

Fig. 4 Excitation (*left*) and emission (*right*) spectra of $BaAl_{2-x}Si_xO_{4-x}N_x$:0.10Eu phosphors with various x ($\lambda_{ex} = 390$ nm, $\lambda_{em} = 500$ nm for $x = 0$; and $\lambda_{ex} = 440$ nm, $\lambda_{em} = 530$ nm for $x = 0.3$–0.8) [54]

excitation band appears for $BaAl_{2-x}Si_xO_{4-x}N_x:Eu^{2+}$ (10 mol.%), peaking at 425–440 nm for x values above 0.3. Correspondingly, the broad emission band shifts to a longer wavelength from 498 to 527 nm up to $x = 0.6$., which can be attributed to increased covalency and crystal field splitting of the 5d state of the Eu^{2+} ions as a consequence of the replacement of O^{2-} by N^{3-}. $BaAl_{2-x}Si_xO_{4-x}N_x:Eu^{2+}$ exhibits a longer wavelength excitation band peaking at about 440 nm, and a green emission at about 500–526 nm ($x = 0.3$). The quantum efficiency of $BaAl_{2-x}Si_xO_{4-x}N_x$:0.10Eu^{2+} ($x = 0.3$) is about 54%, with an excitation wavelength at 460 nm. Consequently, $BaAl_{2-x}Si_xO_{4-x}N_x:Eu^{2+}$ shows high potential as a green-emitting phosphor for pc-white-LEDs applications.

Xie et al. reported the fluorescence of Eu^{2+}-activated $SrSi_5AlO_2N_7$ and $SrSiAl_2O_3N_2$ phosphors with shorter wavelength emission [63]. Both of phosphors show the wide excitation spectrum covering from 250 to 450 nm allowing them to be used as conversion phosphors for white LEDs, and emit blue light peaked at 488 nm for Eu^{2+}-activated $SrSi_5AlO_2N_7$ and 475 nm for $SrSiAl_2O_3N_2:Eu^{2+}$, respectively. In $SrSi_5AlO_2N_7$, Sr^{2+} ions are coordinated by eight (O, N) atoms: two (O, N) at 2.660 Å, two ($N^{[2]}$) at 3.219 Å, and four ($N^{[1]}$) atoms at 3.189 Å [64]. In $SrSiAl_2O_3N_2$, Sr^{2+} ions are coordinated by six O atoms and three N atoms: two ($O^{[1]}$) at 2.807 Å, two ($O^{[2]}$) at 2.634 Å, two ($O^{[3]}$) at 2.887 Å, two ($N^{[1]}$) at 3.114 Å, and one ($N^{[2]}$) at 2.74 Å [65]. The average Sr–(O, N) distance in $SrSi_5AlO_2N_7$ (3.064 Å) or $SrSiAl_2O_3N_2$ (2.862 Å) is longer than that observed in Ca–α-SiAlON (2.606 Å) and $Ca_2Si_5N_8$ (2.652–2.708 Å). The long distances between Eu and (O, N) atoms in these materials is thought to cause weak crystal-field acting on Eu^{2+}, which results in the shorter wavelength emission of Eu^{2+}-activated $SrSi_5AlO_2N_7$ and $SrSiAl_2O_3N_2$.

Eu^{2+}-activated nitridoalumosilicates or nitridosilicates

With respect to Eu^{2+}-activated all-nitride phosphors including nitridoalumosilicates and nitridosilicates, Eu^{2+} photoluminescence varies from blue to deep-red spectral region depending on the composition of host lattices and Eu^{2+} doping concentration. Table 1 summarizes the main luminescence data of these nitrides-based phosphors. In following section, the luminescent properties of

Table 1 Overview of main luminescence data of Eu^{2+}-activated nitride phosphors

Composition	Excitation peaks (nm)	Emission peaks (nm)	Stokes shift (cm^{-1})[d]	References
$CaAlSiN_3:xEu^{2+}$ ($0 < x < 0.20$)	320, 470[a]	650[a]	5860	[66–69]
$(Ca,Sr)AlSiN_3:Eu^{2+}$	300, 420, 470, 560	610–650		[70–73]
$Ca_2Si_5N_8:xEu^{2+}$ ($0 < x < 0.14$)	297, 355, 394, 460, 496[b]	605–615	3800[b]	[76, 80]
$Sr_2Si_5N_8:xEu^{2+}$ ($0 < x < 2.0$)	294, 334, 395, 465, 505[b]	609–680	3700[b]	[76, 80]
$Ba_2Si_5N_8:xEu^{2+}$ ($0 < x < 2.0$)	295, 334, 395, 460, 504[b]	570–680	3500[b]	[76]
HP-$Ca_2Si_5N_8:xEu^{2+}$ ($x = 0.01$)	390[a]	627[a]	9690[a]	[82]
$CaSiN_2:xEu^{2+}$ ($x = 0.03$)	400	605	8470	[84]
$SrSiN_2:xEu^{2+}$ ($0 < x < 0.1$)	306, 336, 395, 466	670–685	6500–6900	[85]
$BaSiN_2:xEu^{2+}$ ($0 < x < 0.1$)	312, 334, 395, 464	600–630	4850–5550	[85]
$LiSi_2N_3:xEu^{2+}$	310	572–584[c]		[86]
$SrYSi_4N_7:Eu^{2+}$	340, 382–386	548, 570	7900–8300	[87, 89]
$BaYSi_4N_7:Eu^{2+}$ ($0.02 < x < 0.40$)	346–349, 383–389	503–537	6200–7200	[88, 89]
$SrSi_6N_8:Eu^{2+}$	310, 370	450	4800	[90]

[a] $x = 0.02$

[b] $x = 0.10$

[c] $x = 0.002$–0.01

[d] Stokes shift calculated from the energy difference between the lowest excitation band and emission wavelength

Eu^{2+}-activated all-nitride-based phosphors including (Ca,Sr)$AlSiN_3$:Eu^{2+} [66–73], $M_2Si_5N_8$:Eu^{2+} (M = Ca, Sr, Ba) [74–81, 83], $MSiN_2$:Eu^{2+} (M = Ca, Sr, Ba) [84, 85], $LiSi_2N_3$:Eu^{2+} [86], $MYSi_4N_7$:Eu^{2+} (M = Sr, Ba) [87–89], and $CaSi_6N_8$:Eu^{2+} [90] are summarized, especially focusing on the composition-dependent luminescent properties.

(Ca,Sr)$AlSiN_3$:Eu^{2+}

Although nitridoalumosilicates $CaAlSiN_3$ with excellent chemical and thermal stabilities was known to be formed in the CaO–AlN–Si_3N_4 phase diagram in 1985 [91], until quite recently $CaSiAlN_3$ was used as host and then a new red-emitting phosphor, Eu^{2+}-doped $CaAlSiN_3$ has been developed [66–69]. Thereupon, the atomic and electronic structure of $CaAlSiN_3$ has been investigated by first-principles pseudopotential method based on density functional theory [92]. Eu^{2+}-doped $CaAlSiN_3$ phosphor owns an extremely broad excitation band covering the range of 250–600 nm, and can be efficiently excited by blue-GaN and near-UV-InGaN LEDs irradiation [66–69]. The emission peak located at around 650 nm, which is assigned to the 5d → 4f transition of Eu^{2+} ion. With increasing of Eu^{2+} concentration, the emission peak of $CaAlSiN_3$:Eu^{2+} was uniformly shifted to longer wavelength (i.e., from 640 to 690 nm). The optimum concentration of the activator Eu^{2+} was reported to be 1.6 and 2.0 mol.% for $CaAlSiN_3$:Eu^{2+} phosphor and its related color coordinates (x, y) are: (0.667, 0.327) and (0.647, 0.347), respectively [66, 68]. In addition, $CaAlSiN_3$:Eu^{2+} maintained 83% of the initial efficiency [67] (or 90% emission intensity at room temperature [68]) above 150 °C. In brief, compared to the other nitride-based phosphors such as $Ca_2Si_5N_8$:Eu^{2+} and $CaSiN_2$:Eu^{2+}, $CaAlSiN_3$:Eu^{2+} phosphor have a higher chemical stability, higher quantum output, and especially a better thermal property, enabling it well suited for high powder pc-white-LEDs. Furthermore, this red-emitting phosphor can compensate the red color deficiency of YAG:Ce^{3+}-based pc-white-LEDs or create white light by combining with a blue LED chip and another green-emitting phosphor. However, when this phosphor is used in conjunction with a green-emitting phosphor, unwanted absorption of the green light might occurs which is difficult to avoid. On the other hand, since the emitting color of $CaAlSiN_3$:Eu^{2+} is somewhat deep-red for lighting applications that require both high color rendering and efficiency, it is desirable to shift the deep-red to orange-reddish color without loss of the quantum output. For this purpose, to weaken the crystal field strength around Eu^{2+} induced by the enlargement of the crystal lattice of $CaAlSiN_3$:Eu^{2+}, substitution of Sr^{2+} (1.32 Å) which has an ionic radius larger than that of Ca^{2+} (1.14 Å) into the Ca^{2+} site of lattice has been proposed [70–73], based on the fact that Sr^{2+} has a good solution capacity in the $CaAlSiN_3$ host lattice to form $Sr_yCa_{1-y}AlSiN_3$ solid solution with the maximum solubility of $y = 0.8$ [71]. As for $Sr_yCa_{1-y}AlSiN_3$:Eu^{2+} phosphors with fixed Eu^{2+}-doping concentration, a blueshift of the red emission peak of Eu^{2+} from 650 to 620 nm (even to 610 nm) by increasing y, was observed [70–73]. Thus, the fine color tuning of (Ca,Sr)$AlSiN_3$:Eu^{2+} can be realized through tailoring the host composition.

$M_2Si_5N_8$:Eu^{2+} (M = Ca, Sr, Ba)

$M_2Si_5N_8$:Eu^{2+} (M = Ca, Sr, Ba) exhibit characteristic of longer wavelength excitation and emission [74–81]. Excitation and emission spectra of these phosphors resemble each other. $M_2Si_5N_8$:Eu^{2+} (M = Ca, Sr) phosphors show typical broadband emission in orange to red spectral region (600–680 nm) depending on the type of M and the Eu^{2+} concentration. $Ba_2Si_5N_8$:Eu^{2+} shows yellow to red emission with maxima from 580 to 680 nm with increasing Eu^{2+} content.

Partial substitution of elements can effectively tune the emission color of Eu^{2+}-doped $M_2Si_5N_8$ (M = Ca, Sr, Ba) series luminescent materials. Within the orthorhombic solid solution $(Ba_{1-a-b}Sr_aCa_b)_2Si_5N_8$:$Eu^{2+}$, the emission peak can be tuned from yellow to deep-red by either increasing the concentration of the smaller sized host lattice cations or by increasing the Eu^{2+} concentration [93]. A complete solution can be formed between isostructural $Ba_2Si_5N_8$ and $Eu_2Si_5N_8$ [94, 95]. Thus, Eu^{2+}-activated $Ba_2Si_5N_8$ with broad excitation band was synthesized [74]. Recently, Piao et al. [75] and Li group [76] reported the luminescence properties of these series phosphors. Under daylight, the body color of phosphors varies from bright yellow to dark red depending on the Eu^{2+} content because of a concomitant shift of the 4f–5d absorption band into the visible region [74, 75]. In the case of higher Eu^{2+}-doping content, the fluorescence intensity of $Ba_{2-x}Si_5N_8$:xEu^{2+} phosphors increases with x and reaches a maximum at $x \sim 0.5$. While, at lower Eu^{2+} content, the maximum intensity was found at $x = 0.04$. As x increases, the emission peak shifts to longer wavelengths, which may be attributed to following three factors: the energy transfer, crystal field strengthening, and re-absorption of the high energy emission.

Only partial crystalline solid solutions can be formed between $Ca_2Si_5N_8$ and $Sr_2Si_5N_8$ compounds with a maximum solubility of Ca at about $x = 0.5$ for $(Sr_{1-x}Ca_x)_2Si_5N_8$:Eu^{2+} (2 atom%) (atom% abbreviated as at.% hereafter) [77]. The first [$Ca_2Si_5N_8$] phase appears at the composition of $x = 0.6$ in $(Sr_{1-x}Ca_x)_2Si_5N_8$. Two phases coexist in the range of $0.5 < x < 0.75$. The partial replacement of Sr by Ca does not significantly change the position of the excitation bands of $Sr_2Si_5N_8$:Eu^{2+} phosphors. As depicted in Fig. 5, in [$Sr_2Si_5N_8$] phase, the emission peaks shift toward

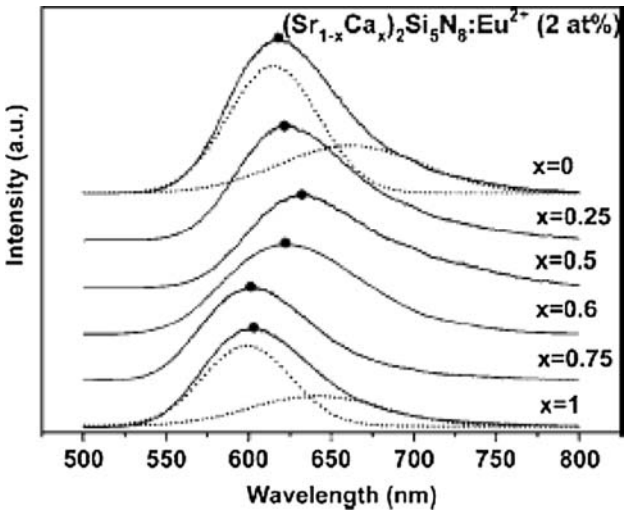

Fig. 5 The dependence of emission spectra of $(Sr_{1-x}Ca_x)_2Si_5N_8:Eu^{2+}$ (2 at.%) on Ca content (x) ($\lambda_{ex} = 405$ nm, The dashed lines show two deconvolved Gaussian subbands peaking at 614, 665 nm for $Sr_2Si_5N_8:Eu^{2+}$ and 598, 642 nm for $Ca_2Si_5N_8:Eu^{2+}$, respectively) [77]

the longer wavelength region when the Ca content is increased up to $x = 0.5$ in $(Sr_{1-x}Ca_x)_2Si_5N_8:Eu^{2+}$ (2 at.%) series. The Eu^{2+} emission band red-shifts from 617 nm for $Sr_2Si_5N_8:Eu^{2+}$ (2 at.%) to 632 nm for $SrCaSi_5N_8:Eu^{2+}$ (2 at.%). Whereas in $[Ca_2Si_5N_8]$ phase, the substitution of Ca by Sr ions results in a weak blue shift of the emission [77]. The red-shifting behavior of emission band can be attributed to the Eu^{2+} ion experiencing a strengthening of crystal field strength caused by changing Ca content in $(Sr_{1-x}Ca_x)_2Si_5N_8:Eu^{2+}$. Another reason for this shifting could be due to an increase of the Stokes shift, which is caused by the shrinkage of Sr sites as Ca is incorporated [80].

$Sr_2Si_5N_8$ and $Eu_2Si_5N_8$ are isostructural with orthorhombic crystal system [94, 95]. Sr^{2+} (1.18 Å, Coordination Number [abbreviated as CN] = 6) and Eu^{2+} (1.17 Å, CN = 6) have a similar ionic size, and Sr–N and Eu–N bonds have almost equivalent bond lengths in the range of 2.60–3.25 Å. Accordingly, with change of Eu^{2+} concentration, excitation spectra of $Sr_2Si_5N_8:Eu^{2+}$ phosphors hardly vary except the intensity. However, emission peak of $Sr_2Si_5N_8:Eu^{2+}$ shifts to the longer wavelength side with increasing the Eu^{2+} concentration [79], due to the increased Stokes shift and re-absorption mechanism. At 150 °C, which the white-LEDs usually works, emission intensity of $Sr_2Si_5N_8:Eu^{2+}$ and $Ba_2Si_5N_8:Eu^{2+}$ remains about 86% [83], 80% [75] of that measured at room temperature, respectively, indicating their low thermal quenching effect. $M_2Si_5N_8:Eu^{2+}$(M = Ca, Sr, Ba) can afford conversion of the blue radiation of LEDs chips into red light, thus, in combination with a green to yellow-emitting phosphors, achieving warm white light pc-white-LEDs with improved color rendition in the red spectral region [83, 93, 96, 97]. Thus, this series luminescent materials are now being industrially used in pc-white-LEDs as highly efficient red-emitting phosphors [83, 97].

$MSiN_2:Eu^{2+}$ (M = Ca, Sr, Ba)

Efficient excitation and high absorption in the near-UV and green spectral region of $MSiN_2:Eu^{2+}$ (M = Ca, Sr, Ba) phosphors perfectly make them match with the radiative from the InGaN or GaN LEDs chips. Under 400 nm excitation, $MSiN_2:Eu^{2+}$ (M = Ca, Sr, Ba) show a broad-band emission in the spectral range from orange to deep-red (600–690 nm) [84, 85]. The position of their excitation peaks is not largely dependent on the type of the M and Eu^{2+} concentration. Only a small variation for Sr versus Ba can be observed. When the Eu^{2+} concentration changes, the excitation spectrum hardly varies except for intensity. The emission of $SrSiN_2:Eu^{2+}$ is located at a lower energy than that of $BaSiN_2:Eu^{2+}$. Two kinds of effects (i.e., crystal field strength and Stokes shift) may be able to explain this phenomenon [85]. First, the crystal field strength and 5d splitting are larger for Eu^{2+} in $SrSiN_2$ than that in $BaSiN_2$, due to smaller metal–ligand (Eu–N) distance in $SrSiN_2:Eu^{2+}$ than in $BaSiN_2:Eu^{2+}$. Second, the Stokes shift for Eu^{2+} on Sr^{2+} site is larger than that on Ba^{2+} site in isostructural host compounds. The red shift of emission peaks of $MSiN_2:Eu^{2+}$ (M = Sr, Ba) phosphors with increasing of Eu^{2+} content is also observed. Thus, the tunable luminescent properties of $(Sr,Ba)SiN_2:Eu^{2+}$ phosphor by changing the mole ratio of Sr/Ba at fixed Eu^{2+} concentration or tuning Eu^{2+} doping concentration, is favorable for developing new phosphors for pc-white-LEDs applications.

$LiSi_2N_3:Eu^{2+}$

Because the nearest Li^+–Li^+ distance in $LiSi_2N_3$ lattice (~2.8 Å) is slightly larger than the ionic size of Eu^{2+} (2.34 Å, CN = 6), which is suitable for the occupation of RE ions such as Eu^{2+} and Ce^{3+}, etc., $LiSi_2N_3$ is used as a host for phosphor. More recently, Li and coworkers reported the photoluminescence properties of RE-doped $LiSi_2N_3$ [86]. They found that the partial replacement of $(LiSi)^{5+}$ with $(CaAl)^{5+}$ results in a large red shift of the emission peak for $Li_{1-2x-y}Ca_yEu_xSi_{2-y}Al_yN_3$ from yellow (~580 nm) to red spectral region (~620 nm). No obvious changes for the excitation spectra by this partial replacement occurs, implying very limited changes in the crystal field splitting and the center of gravity of Eu^{2+} 5d excitation states. In addition, the luminescence intensity is significantly increased, showing high potential for white-LEDs applications. These results testified again that double

substitution is an effective way to improve and modify the luminescence properties of (oxy)nitrides-based phosphors, which provides opportunities for the design of conversion materials in pc-white-LEDs.

$MYSi_4N_7:Eu^{2+}$ (M = Sr, Ba)

$SrYSi_4N_7$, $BaYSi_4N_7$, and $EuYSi_4N_7$ are isostructural with the hexagonal symmetry. Considering the comparable ionic radii and isovalence of Sr^{2+}, Ba^{2+}, and Eu^{2+} ions, it is expected that Eu^{2+} ions prefer to occupy Sr or Ba sites in corresponding hosts (i.e., $SrYSi_4N_7$ and $BaYSi_4N_7$). Therefore, the emission peak and efficiencies can be tuned through varying the Eu concentration [89]. The excitation spectra of $MYSi_4N_7:Eu^{2+}$ (M = Sr, Ba) series phosphor show broadband ranging from UV to blue region, matching the radiation of near-UV GaN LED chips, which makes this series phosphors promising for pc-white-LEDs application. Under excitation of near-UV light, $MYSi_4N_7:Eu^{2+}$ (M = Sr, Ba) series phosphors exhibit yellow and green fluorescence for M = Sr, and Ba, respectively. And the emission peaks varied from type of alkaline earth and Eu content. The emission peak of $SrYSi_4N_7:Eu^{2+}$ is at lower energy (i.e., longer wavelength) than that of $BaYSi_4N_7:Eu^{2+}$. With increasing Eu content, the excitation peak as well as emission band shift to longer wavelength, which is mainly ascribed to the change of the crystal field strength and Stokes shift.

$CaSi_6N_8:Eu^{2+}$

Shorter wavelength emission of Eu^{2+} was also observed in $SrSi_6N_8:Eu^{2+}$ [90]. This phosphor shows the wide excitation spectrum covering from 250 to 430 nm, and emits pure-blue light peaked at 450 nm. In $SrSi_6N_8$ host lattice, Sr^{2+} ions are tenfold coordinated to N^{3-} anions (versus sixfold coordination in $M_2Si_5N_8$ (M = Ca, Sr, and Ba), sevenfold coordination in Ca–α-SiAlON) at distances of 2.69–3.16 Å [98], longer than that observed in Ca–α-SiAlON (2.606 Å) and $Ca_2Si_5N_8$ (2.652–2.708 Å). As the cation radii of Eu^{2+} and Sr^{2+} are very close to each other, Eu^{2+} ions substitute for Sr^{2+} sites and ten-coordinated by N^{3-} anions in $SrSi_6N_8$ host lattice. The larger metal–ligand distances in $SrSi_6N_8$ results in weaker crystal field strength, which is similar to the cases in Eu^{2+}-activated $SrSi_5AlO_2N_7$ and $SrSiAl_2O_3N_2$. As a consequence, shorter wavelength emission of $SrSi_6N_8:Eu^{2+}$ occurs. The above examples of Eu^{2+}-activated (oxy)nitrides with shorter wavelength emission suggest that (oxy)nitrides with the large CN of M metals such as $SrSi_6N_8$ (CN = 10) [90], $SrSiAl_2O_3N_2$ (CN = 9) [63], and $SrSi_5AlO_2N_7$ (CN = 8) [63], can be designed as blue-emitting phosphor for pc-white-LEDs.

Ce^{3+}-activated nitride and oxynitride phosphors

Ce^{3+} with the electronic configuration $4f^1$, has $^2F_{7/2}$ and $^2F_{5/2}$ manifolds as the ground states separated by $\sim$2,000 cm^{-1} due to spin–orbit coupling. The lower manifold $^2F_{5/2}$ is populated and the manifold $^2F_{7/2}$ is almost empty at room temperature. The excited configuration is 5d which is split by the crystal field in 2–5 components. As the positions of the energy levels of 5d excited states of Ce^{3+} are not only affected by the symmetry and strength of the crystal field but also by the degree of covalent bonding, it causes variations in the absorption and emission from UV to longer wavelength by varying the host lattice. Hence, most Ce^{3+}-activated phosphors show broadband emission in the UV and visible ranges due to the $4f^05d^1$–$4f^1$ transition of Ce^{3+} [3, 4, 11]. In this section, the tunable luminescent properties of Ce^{3+}-activated nitrides and oxynitrides will be reviewed. The relationship between the composition and luminescence properties of these phosphors will be specifically addressed.

Ce^{3+}-doped α-SiAlON

Ce^{3+}-doped α-SiAlON longer wavelength luminescent materials were first synthesized by Hintzen and coworkers [99]. Thereafter, Xie et al. [100] prepared Ce^{3+}-doped Ca–α-SiAlON phosphors with the compositions of $(Ca_{1-3/2x}Ce_x)_{m/2}Si_{12-m-n}Al_{m+n}O_nN_{16-n}$ ($0.5 \le m \le 3.0$, $m = 2n$). With increasing m and x values, the emission peak red shifts (See Fig. 6a, b). The PL intensity of the Ce^{3+}-doped Ca–α-SiAlON phosphor is strongly related to the composition of the host lattice (i.e., the m values). Besides the changes in the emission intensity with varying m values, a red shift of the emission wavelength occurs in the Ce^{3+}-doped sample as m values increases. As for the reason of this upward shift, it is highly possible that higher m values lower the emission energy for transfer from the low 5d excited state to the 4f ground state, and therefore shift the emission peak to a longer wavelength [100].

Similarly, red shift of emission peak is also observed in Ce^{3+}-doped α-SiAlON phosphors, as Ce^{3+} concentration increases [100]. The position of emission spectrum shifts from 485 to 503 nm when the Ce^{3+} concentration rises from 5 to 25 at.%. This upward shift perhaps results from the re-absorption process with high Ce^{3+} content, which reduces the emission at the blue wing [100]. Ce^{3+}-doped Ca–α-SiAlON phosphor can be excited efficiently by ultraviolet LEDs with the primary emission wavelength of 365–380 nm, which is suitable for use in pc-white-LEDs.

Ce^{3+}-activated oxynitrides

In 1998, van Krevel group reported longer wavelength emission of Ce^{3+} in Y–Si–O–N materials such as

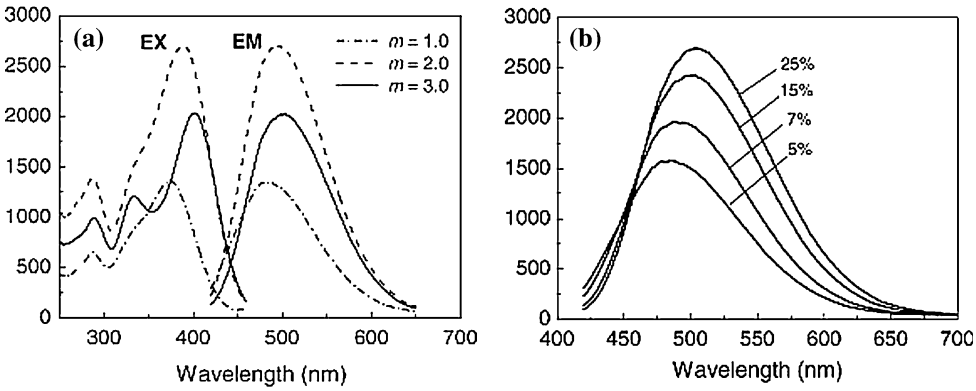

Fig. 6 **a** Excitation ($\lambda_{em} = 495$ nm) and emission spectra ($\lambda_{ex} = 390$ nm) of 10 at.% Ce^{3+}-doped Ca–α-SiAlON phosphors; **b** Emission spectra of Ce^{3+}-doped Ca–α-SiAlON phosphors with different doping concentration ($m = 2.0$) [100]

Ce^{3+}-doped $Y_5(SiO_4)_3N$, $Y_4Si_2O_7N_2$, $YSiO_2N$, and $Y_2Si_3O_3N_4$. It is well-known that conversion phosphors for pc-white-LEDs have to efficiently absorb in the near-UV to blue spectral range and emit light in the visible. Among the above oxynitrides, $Y_4Si_2O_7N_2$:Ce^{3+} and $Y_2Si_3O_3N_4$:Ce^{3+} materials could be used as phosphors for white-LEDs because their excitation spectra extending from UV to about 460 nm match the output wavelength of LEDs chips [45]. As a multinary covalent oxynitride compound, $LnAl(Si_{6-z}Al_z)(N_{10-z}O_z)$ (Ln = La, Ce, $z \sim 1$), was early studied as heat-resistant ceramic materials [101]. Recently, in order to find a blue-emitting phosphor that can be excited in the near-UV range around 405 nm and have little thermal degradation, Ce^{3+}-activated $LaAl(Si_{6-z}Al_z)(N_{10-z}O_z)$ ($z \sim 1$) (termed as JEM:Ce^{3+}) phosphors were designed and synthesized [102]. As shown in Fig. 7a and b, JEM:Ce^{3+} phosphors are applicable for 405 nm excitation, and emit strong blue-to-blue-green colors with varying Ce^{3+} content. With the increase of Ce^{3+} concentration, both the excitation and emission bands shifted towards longer wavelength side. At the same time, the excitation spectra tend to be broadened. As the Ce^{3+} concentration increase, intensities at the excitation wavelength of 405 nm, at which the efficiency of InGaN LED chips is believed to be the highest, also tend to increase. The emission peak varies in a range of over 30 nm while the intensity remains high, even for the sample with $x = 1$. This remarkable change of luminescence peaks with varying Ce content is supposed to be due to the change of ligand fields around activator ions. These results indicate that the optical properties of JEM:Ce^{3+} can be tunable by changing its host composition or Ce^{3+}-doping content. The Full Width at Half Maximum of JEM:Ce^{3+} is more than 110 nm, which allows us to achieve good color rendering of illuminations. The external quantum efficiency (50%) of JEM:Ce^{3+} phosphor is higher than that of a commercially available blue-emitting phosphor BAM:Eu^{2+} with the values of 46% when measured at 405 nm excitation. The luminous efficiency of white LEDs fabricated by InGaN chip with JEM:0.5Ce^{3+}, $CaAlSiN_3$:Eu^{2+}(red), α-SiAlON (yellow), and β-SiALON (green) phosphor blends under a drive current of 20 mA varies from 19 to 20 lm/W, which is comparable to that of conventional tungsten illumination values. High color rendering index was reported to be >95 in white LEDs with various correlated color temperatures [102], indicating the suitability of the JEM:Ce^{3+} phosphor in solid-state lightings.

Ce^{3+}-activated nitridoalumosilicates or nitridosilicates

$CaAlSiN_3$:Ce^{3+}

As indicated above, within the all-nitride host of $CaAlSiN_3$, the lowest of 5d excitation bands of Eu^{2+} is extended up to 450–500 nm by highly covalent Ca–N bond and strong crystal field on the Ca site [66–69]. Similar to the case of

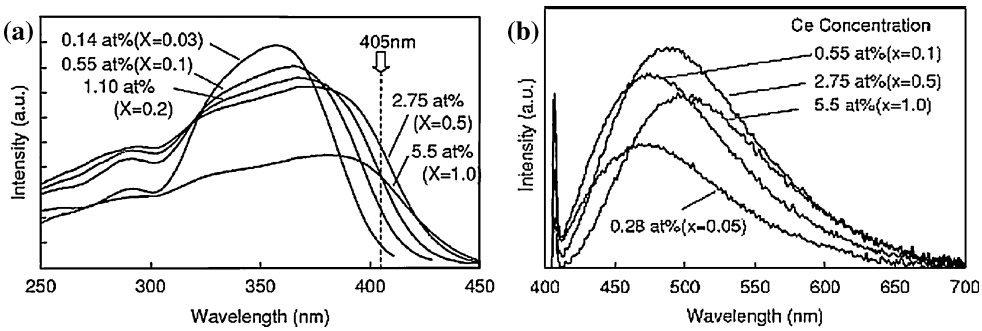

Fig. 7 Excitation (**a**) and emission (**b**, $\lambda_{ex} = 405$ nm) spectra of $La_{1-x}Ce_xAl(Si_{6-z}Al_z)(N_{10-z}O_z)$ ($z \sim 1$) phosphors with various Ce^{3+} concentration (x) [102]

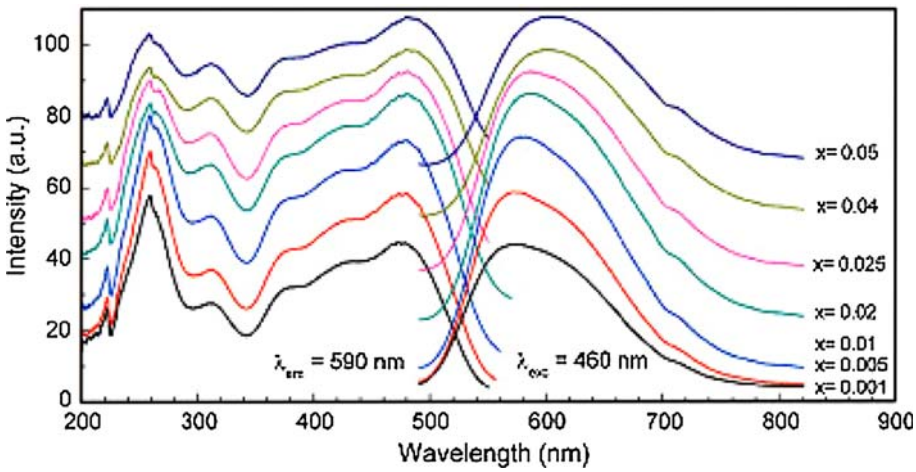

Fig. 8 Excitation (*left*, $\lambda_{em} = 590$ nm) and emission (*right*, $\lambda_{ex} = 460$ nm) spectra of $Ca_{1-2x}Ce_xLi_xAlSiN_3$ phosphors (Li^+ as the charge compensator) with different Ce^{3+} concentration ($0.001 \leq x \leq 0.05$) [103]

Eu^{2+} ion, the 5d excitation band of Ce^{3+} also presented in the visible range in $CaAlSiN_3$ host reported by Li et al. [103]. As shown in Fig. 8, $CaAlSiN_3:Ce^{3+}$, Li^+ phosphors can be efficiently excited by blue light (450–480 nm) and yield yellow-orange emission with a broadband peaking in the range of 570–603 nm, originating from the $5d^1 \rightarrow 4f^1$ transition of Ce^{3+}. The position of excitation band is nearly independent of Ce^{3+} content in spite of the longest excitation band at about 480 nm, just showing a slight red-shift of about 6 nm, i.e., 474–480 nm starting from $x = 0.001$ and stopping at $x = 0.02$. However, as increasing Ce^{3+} concentration, the emission band of Ce^{3+} shifts toward longer wavelengths from 570 to 603 nm with increasing Ce^{3+} content from $x = 0.001$–0.05, which can be ascribed to the increased Stokes shift corresponding to structural relaxation and energy transfer of Ce^{3+}. Upon excitation in blue light range (450–480 nm), the internal and external quantum efficiency of $CaAlSiN_3:Ce^{3+}$ can be reached above 70 and 50%, respectively. Furthermore, $CaAlSiN_3:Ce^{3+}$ is very stable against temperature up to 300 °C in air. Using $CaAlSiN_3:Ce^{3+}$ as conversion phosphor combined with a blue InGaN LED-chip (450 nm), warm white-LEDs can be generated, yielding the luminous efficacy of about 50 lm/W at color temperature 3,722 K and the color rendering index (R_a) of 70.

$M_2Si_5N_8:Ce^{3+}$ (M = Ca, Sr, Ba)

As mentioned above, Ce^{3+}-doped oxynitrides show very interesting luminescence properties and the Ce^{3+} emission peak can be varied over a large spectral range with change of chemical composition or Ce^{3+} concentration [100, 102]. With respect to all-nitride phosphors, another interesting nitride host is $M_2Si_5N_8$ (M = Ca, Sr, Ba) for which Eu^{2+} luminescence has been reported [74–81, 83]. Li et al. [104] reported the luminescence properties of Ce^{3+}-activated $M_2Si_5N_8$ (M = Ca, Sr, Ba) codoped with charge compensator Li^+ or Na^+ ions. It is found that the excitation bands of $M_2Si_5N_8:Ce^{3+}$, Li^+ (M = Ca, Sr) phosphors perfectly match the UV–blue light radiation of (In,Ga)N LEDs chips in the range of 370–450 nm. Table 2 gives the main luminescence data of $M_2Si_5N_8:Ce^{3+}$, A^+ (M = Ca, Sr, Ba, A = Li, Na) series phosphors. Ce^{3+}-activated $M_2Si_5N_8$ phosphors exhibit broad emission bands with

Table 2 Summary of main luminescence data of $M_2Si_5N_8:Ce^{3+}$, A^+ (M = Ca, Sr, Ba, A = Li, Na) series phosphors [104]

Composition	Excitation bands (nm)	Emission bands (nm)	Stokes shift (cm^{-1})
$Ca_2Si_5N_8$:Ce,Li	261, 288, 329, 365, 397	470	3700
$Ca_2Si_5N_8$:Ce,Na	260, 286, 329, 373, 396	471	3700
$Sr_2Si_5N_8$:Ce,Li	260, 276, 330, 387, 431 (Ce_{Sr1})	495 (Ce_{Sr1})	2600
	259, 272, 327, 395 (Ce_{Sr2})	553 (Ce_{Sr2})	6700
$Sr_2Si_5N_8$:Ce,Na	260, 279, 328, 396, 434 (Ce_{Sr1})	520 (Ce_{Sr1})	2700
	261, 280, 326, 395 (Ce_{Sr2})	556 (Ce_{Sr2})	7000
$Ba_2Si_5N_8$:Ce,Li	260, 284, 384, 415 (Ce_{Ba1})	451, 497 (Ce_{Ba1})	2000
	257, 285, 380, 405 (Ce_{Ba2})	561 (Ca_{Ba2})	6400
$Ba_2Si_5N_8$:Ce,Na	258, 285, 384, 416 (Ce_{Ba2})	457, 495 (Ce_{Ba1})	2100
	259, 286, 384, 406 (Ce_{Ba2})	560 (Ce_{Ba2})	6400

Stokes shift calculated from the energy difference between the lowest excitation band and emission wavelength

maxima at 470, 553, and 451 nm for M = Ca, Sr, Ba, respectively, due to the 5d–4f transition of Ce^{3+}. $M_2Si_5N_8$:Ce^{3+},Li^+ (M = Sr, Ba) obviously shows two Ce^{3+} emission centers due to the fact that the Ce^{3+} ions occupy two M sites. With increasing Ce^{3+} concentration, both absorption and emission intensity increase and the position of the emission bands show a slight red-shift (<10 nm). The maximum solubility of Ce^{3+} in $M_2Si_5N_8$ is about 2.5 mol.% ($x \approx 0.05$) for both $Ca_2Si_5N_8$ and $Sr_2Si_5N_8$. With increasing the ionic radius going from Ca to Sr and Ba, the ratio of emission intensity to absorption intensity of Ce^{3+} decreases related to a decreasing Ce^{3+} solubility. In addition, the influence of using Na^+ instead of Li^+ ion as charge compensator on emission and excitation properties is small but Na^+ enhances the emission intensity because of larger solubility of Ce^{3+} in $M_2Si_5N_8$ (M = Ca, Sr).

$MSiN_2$:Ce^{3+} (M = Ca, Sr, Ba)

Under excitation of near-UV light, $CaSiN_2$:Ce^{3+} and $MSiN_2$:Ce^{3+},Li^+ (M = Sr, Ba) phosphors exhibit a broad emission band in the wavelength range of 400–700 nm with a peak center at 625, 535, and 485 nm for $CaSiN_2$, $SrSiN_2$, and $BaSiN_2$, respectively [84, 85]. The excitation band of $CaSiN_2$:Ce^{3+} has a maximum around 535 nm and extends from 425 to 575 nm. Under excitation of 535 nm green light, this phosphor emits intense red luminescence with broad emission band. The luminescence properties of Ce^{3+}-activated $CaSiN_2$ vary with the substitution of Ca by Sr and Mg, or Si by Al [84]. It is observed that Sr substitution on the Ca site leads to a red shift of the emission peak. But Mg substitution on the Ca site results in the emission peak shifting to shorter wavelength. The excitation peak blue-shifts, too, from a maximum at 535 to 475 nm for 10% Al substitution. At the same time, the emission peak shifts from 625 to 560 nm. With the Al substitution, therefore, this compound becomes interesting as a yellow phosphor for white-LEDs application with a blue (around 460 nm) LEDs chip. As respect to $MSiN_2$:Ce^{3+},Li^+ (M = Sr, Ba), similar to the cases of Eu^{2+} in $SrSiN_2$ and $BaSiN_2$ host lattice, Ce^{3+} also shows a larger Stokes shift and longer wavelength emission in $SrSiN_2$ than in the $BaSiN_2$ [85].

Yb^{2+}-doped α-SiAlON phosphor

Yb^{2+} ion is one of RE activators for a variety of optical crystals used in tunable solid-state lasers [105]. The observed optical spectra of Yb^{2+} are considered to originate from electronic transitions between ground state $4f^{14}$ and $4f^{13}5d^1$ excited state. So far, the studies of the fluorescence properties of Yb^{2+} have concentrated mostly on alkaline earth halides, fluorides, silicates, sulfates, phosphates, aluminates, and haloapatites [105]. Compared with many studies on Eu^{2+} or Ce^{3+}-activated (oxy)nitrides, there are few reports on Yb^{2+} doped (oxy)nitrides. Recently, Xie et al. investigate the luminescence properties of Yb^{2+}-doped α-SiAlON green-emitting phosphor for white LEDs with the compositions of $(M_{1-2x/v}Yb_x)_{m/v}Si_{12-m-n}Al_{m+n}O_nN_{16-n}$ (M = Ca, Li, Mg, and Y, v is the valency of M, $0.002 \leq x \leq 0.10$, $0.5 \leq m = 2n \leq 3.5$) [106]. The effect of modifying cations (i.e., Ca, Li, Mg, and Y) on the luminescence properties of Yb^{2+}-doped α-SiAlON was also studied [106]. The luminescence spectra of these α-SiAlONs strongly resemble each other, suggesting that the coordination of Yb^{2+} ions remains the same for all α-SiAlONs. The luminescence efficiency of Yb^{2+} in Ca–α-SiAlON is about two and six times higher than that of Yb^{2+} in Li– and Mg–α-SiAlON, respectively. The emission of Yb^{2+} in Y–α-SiAlON is very weak and is not visible to the naked eye. The maximal emission of Yb^{2+} in Li–, Mg–, and Ca–α-SiAlONs is situated at 537, 543, and 549 nm, respectively. Ca–α-SiAlON:Yb^{2+} phosphor shows intense green emission centered at 549 nm under the excitation of 450–470 nm at which blue LEDs usually work. The CIE chromatic coordinations are $X = 0.323$ and $Y = 0.601$ for Ca–α-SiAlON:Yb^{2+} phosphor, which shows better color saturation than commercially available BAM:Eu^{2+},Mn^{2+} green-emitting phosphor and is close to that of ZnS:Cu,Al phosphor.

Summary and outlook

In summary, the fluorescence properties of (oxy)nitride-based luminescent materials doped by Eu^{2+}, Ce^{3+}, and Yb^{2+}, are described with the emphasis on the dependence of luminescence properties on composition. Because of their compositional and structural versatilities, (oxy)nitride luminescent materials with desired excitation range and emission color can be obtained by varying the composition of host or RE activator. For the design of efficient nitride and oxynitride-based phosphors for white LEDs, the following aspects should be taken into account: (1) Based on the phase diagrams of nitrides or oxynitrides, forming solid solution by chemical elements substitution is an important method to modify the composition and then the crystal field for better energy match and more efficient energy transfer; (2) The nitride or oxynitride hosts with high vibrational frequency should be selected, because the Stokes shift is expected to be smaller in phosphors whose vibrational frequencies are so high that only the ground vibrational state can be occupied; (3) Since phosphor powders consisting of highly spherical particles can increase the packaging density and surface

uniformity to apply for pc-white-LEDs devices, suitable morphology and particle size, especially monodisperse spherical particle with size no more than 5 um are required; (4) Energy saving and environmental friendly methods of materials synthesis which can be scaled up for industrial applications, should be developed; (5) The performance of the state-of-the-art nitride and oxynitride phosphors for pc-white-LEDs, especially blue-emitting phosphors, is still not good enough for practical application. Thus, it is urgent to seek for suitable and efficient blue-emitting phosphors for pc-white LEDs application.

Acknowledgements This work was supported by the Natural Science Research Project of the Jiangsu Higher Education Institutions (08KJD150014) and QingLan Project of the Jiangsu Province, China (2008).

References

1. Nakamura S, Fasol G (1996) The blue laser: GaN based light emitters and lasers. Springer, Berlin
2. Jüstel T, Nikel H, Ronda C (1998) Angew Chem Int Ed 37:3084
3. Shionoya S, Yen WM (1999) Phosphor handbook. CRC Press, New York
4. Xu R, Su M (2004) Luminescence and luminescent materials. Chemical Industry Press, Beijing (In Chinese)
5. Schubert EF, Kim JK (2005) Science 308:1274
6. Phillips JM, Coltrin ME, Crawford MH, Fischer AJ, Krames MR, Regina M-M, Mueller GO, Ohno Y, Rohwer LES, Simmons JA, Tsao JY (2007) Laser Photon Rev 1(4):307
7. Luo X, Cao W, Sun F (2008) Chinese Sci Bull 53(19):2923
8. Yang WJ, Luo LY, Chen TM, Wang NS (2005) Chem Mater 17:3883
9. Jang HS, Yang HS, Kim SW, Han JY, Lee SG, Jeon DY (2008) Adv Mater 20:2696
10. He XH, Zhu Y (2008) J Mater Sci 43(5):1515
11. Blasse G, Grabmaier BC (1994) Luminescent materials. Springer, Berlin
12. Setlur AA, Heward WJ, Hannah ME, Happek U (2008) Chem Mater 20:6277
13. Lu CH, Jagannathan R (2002) Appl Phys Lett 80(19):3608
14. Kong L, Gan S, Hong G, You H, Zhang J (2008) Chem J Chinese Univ 29(4):673
15. Xie RJ, Hirosaki N (2007) Sci Technol Adv Mater 8:588
16. Luo X (2008) J Chin Ceram Soc 36(9):1335 (In Chinese)
17. Yamada T, Yamao T, Sakata S (2007) Key Eng Mater 352:173
18. Hampshire S, Park HK, Thompson DP, Jack KH (1978) Nature 274:880
19. Ekstrom T, Nygren M (1992) J Am Ceram Soc 75:259
20. Cao GZ, Metselaar R (1991) Chem Mater 3:242
21. Karunaratne BSB, Lumby RJ, Lewis MH (1996) J Mater Res 11(11):2790
22. Shen ZJ, Nygren M, Halenius U (1997) J Mater Sci Lett 16:263
23. Xie RJ, Hirosaki N, Sakuma K et al (2004) Appl Phys Lett 84(26):5404
24. Xie RJ, Hirosaki N, Mitomo M et al (2004) J Phys Chem B 108:12027
25. Sakuma K, Hirosaki N, Xie RJ (2007) J Lumin 126:843
26. Jang Y, Park JS, Kim JS, Han SO, Kim HS, Ahn YS, Yoo SJ. J Electroceram. doi:10.1007/s10832-008-9446-x
27. Sakuma K, Hirosaki N, Xie RJ, Yamamoto Y, Suehiro T (2006) Phys Stat Sol (c) 3(8):2701
28. Sakuma K, Hirosaki N, Xie RJ, Yamamoto Y, Suehiro T (2007) Mater Lett 61:547
29. Xie RJ, Hirosaki N, Mitomo M, Sakuma K, Kimura N (2006) Appl Phys Lett 89:241103
30. Xie RJ, Hirosaki N, Mitomo M, Takahashi K, Sakuma K (2006) Appl Phys Lett 88:101104
31. Mandal H, Hoffmann MJ (1999) J Am Ceram Soc 82(1):229
32. Mitomo M, Ishida A (1999) J Eur Ceram Soc 19:7
33. Mandal H, Thompson DP, Ekstrom T (1993) J Eur Ceram Soc 12:421
34. Shen Z, Ekstrom T, Nygren M (1996) J Eur Ceram Soc 16:873
35. Mandal H, Thompson DP (1999) J Eur Ceram Soc 19:543
36. Oyama Y, Kamigaito O (1971) Jpn J Appl Phys 10:1637
37. Jack KH, Wilson WI (1972) Nat Phys Sci (London) 238:28
38. Jack KH (1976) J Mater Sci 11:1135. doi:10.1007/BF02396649
39. Ekstrom T, Nygren M (1992) J Am Ceram Soc 75(2):259
40. Petzow G, Herrmann M (2002) Struct Bonding 102:47
41. Hirosaki N, Xie RJ, Kimoto K, Sekiguchi T, Yamamoto Y, Suehiro T, Mitomo M (2005) Appl Phys Lett 86:211905
42. Xie RJ, Hirosaki N, Li HL, Li YQ, Mitomo M (2007) J Electrochem Soc 154(10):J314
43. Kimura N, Sakuma K, Hirafune S, Asano K, Hirosaki N, Xie RJ (2007) Appl Phys Lett 90:051109
44. Zhou Y, Yoshizawa Y, Hirao K et al (2008) J Am Ceram Soc 91(9):3082
45. van Krevel JWH, Hintzen HT, Metselaar R, Meijerink A (1998) J Alloys Compd 268:272
46. Li YQ, Delsing ACA, de With G, Hintzen HT (2005) Chem Mater 17:3242
47. Yun BG, Miyamoto Y, Yamamoto H (2007) J Electrochem Soc 154(10):J320
48. Bachmann V, Jüstel T, Meijerink A, Ronda C, Schmidt PJ (2006) J Lumin 121:441
49. Yun BG, Machida K, Yamamoto H (2007) J Ceram Soc Jpn 115(10):619
50. Zhang M, Wang J, Zhang Z, Zhang Q, Su Q (2008) Appl Phys B 93:829
51. Bachmann V, Ronda C, Oeckler O, Schnick W, Meijerink A (2009) Chem Mater 21(2):316
52. Liu RS, Liu YH, Bagkar NC, Hu SF (2007) Appl Phys Lett 91:061119
53. Hölsä J, Jungner H, Lastusaari M, Niittykoski J (2001) J Alloys Compd 323–324:326
54. Li YQ, With GD, Hintzen HT (2006) J Electrochem Soc 153(4):G278
55. Hőppe HA, Stadler F, Oeckler O, Schnick W (2004) Angew Chem Int Ed 43:5540
56. Stadler F, Oeckler O, Hőppe HA, Mçller MH, Pçttgen R, Mosel BD, Schmidt P, Duppel V, Simon A, Schnick W (2006) Chem Eur J 12:6984
57. Oeckler O, Stadler F, Rosenthal T, Schnick W (2007) Solid State Sci 9:205
58. Kechele JA, Oeckler O, Stadler F, Schnick W (2009) Solid State Sci 11:537
59. Hintzen HT, Li YQ (2004) World Patent WO2004/029177A1
60. Fiedler T, Fries T, Jermann F, Zachau M, Zwaschka F (2005) World Patent WO2005/061659A1
61. Schmidt PJ, Mayr W, Meyer J, Schreinemacher B (2006) World Patent WO2006/095284A1
62. Lin YS, Tseng YH, Liu RS, Chan JCC (2007) J Electrochem Soc 154(2):P16
63. Xie RJ, Hirosaki N, Yamamoto Y, Suehiro T, Mitomo M, Sakuma K (2005) J Ceram Soc Jpn 13(7):462

64. Shen Z, Grins J, Esmaeilzadeh S, Ehrenberg H (1999) J Mater Chem 9:1019
65. Lauterbach R, Schnick W (1998) Z Anorg All Chem 624(7):1154
66. Uheda K, Hirosaki N, Yamamoto Y, Naito A, Nakajima T, Yamamoto H (2006) Electrochem Solid State Lett 9(4):H22
67. Uheda K, Hirosaki N, Yamamoto H (2006) Phys Stat Sol (a) 203(11):2712
68. Piao X, Machida K, Horikawa T, Hanzawa H, Shimomura Y, Kijima N (2007) Chem Mater 19:4592
69. Li J, Watanabe T, Wada H, Setoyama T, Yoshimura M (2007) Chem Mater 19:3592
70. Mikami M, Watanabe H, Uheda K, Shimooka S, Shimomura Y, Kurushima T, Kijima N (2009) IOP Conf Ser Mater Sci Eng 1:012002
71. Watanabe H, Wada H, Seki K, Itou M, Kijima N (2008) J Electrochem Soc 155(3):F31
72. Watanabe H, Kijima N (2009) J Alloys Compd 475:434
73. Watanabe H, Yamane H, Kijima N (2008) J Solid State Chem 181:1848
74. Hőppe HA, Lutz H, Morys P, Schnick W, Seilmeier A (2000) J Phys Chem Solids 61:2001
75. Piao X, Machida K, Horikawa T, Hanzawa H (2007) Appl Phys Lett 91:041908
76. Li YQ, van Steen JEJ, van Krevel JWH, Botty G, Delsing ACA, DiSalvo FJ, de With G, Hintzen HT (2006) J Alloys Compd 417:273
77. Piao X, Horikawa T, Hanzawa H, Machida K (2006) J Electrochem Soc 153(12):H232
78. Piao X, Horikawa T, Hanzawa H, Machida K (2006) Appl Phys Lett 88:161908
79. Xie RJ, Hirosaki N, Suehiro T, Xu FF, Mitomo M (2006) Chem Mater 18:5578
80. Li YQ, de With G, Hintzen HT (2008) J Solid State Chem 181(3):515
81. Zeuner M, Hintze F, Schnick W (2009) Chem Mater 21:336
82. Römer SR, Braun C, Oeckler O, Schmidt PJ, Kroll P, Schnick W (2008) Chem Eur J 14:7892
83. Xie RJ, Hirosaki N, Kimura N, Sakuma K, Mitomo M (2007) Appl Phys Lett 90:191101
84. Toquin RL, Cheetham AK (2006) Chem Phys Lett 423:352
85. Duan CJ, Wang XJ, Otten WM, Delsing ACA, Zhao Z, Hintzen HTJM (2008) Chem Mater 20:1597
86. Li YQ, Hirosaki N, Xie RJ, Takeka T, Mitomo M (2008) J Solid State Chem. doi:10.1016/j.jssc.2008.10.031
87. Li YQ, Fang CM, de With G, Hintzen HT (2004) J Solid State Chem 177:4687
88. Li YQ, de With G, Hintzen HT (2004) J Alloys Compd 385:1
89. Li YQ (2005) Structure and luminescence properties of novel rare-earth doped silicon nitride based materials. PhD Thesis, Eindhoven University of Technology
90. Shioi K, Hirosaki N, Xie RJ, Takeda T, Li YQ (2008) J Mater Sci 43:5659. doi:10.1007/s10853-008-2764-1
91. Huang Z, Sun W, Yan D (1985) J Mater Sci Lett 4:255
92. Mikami M, Uheda K, Kijima N (2006) Phys Stat Sol (a) 203:2705
93. Regina MM, Mueller G, Krames MR, Höppe HA, Stadler F, Schnick W, Juestel T, Schmidt P (2005) Phys Stat Sol (a) 202:1727
94. Huppertz H, Schnick W (1997) Acta Crystallogr C 53:1751
95. Schlieper T, Milius W, Schnick W (1995) Z Anorg Allg Chem 621:1380
96. Yamada M, Naitou T, Izuno K, Tamaki H, Murazaki Y, Kameshima M, Mukai T (2003) Jpn J Appl Phys 42:L20
97. Schmidt P, Tuecks A, Meyer J, Bechtel H, Wiechert D, Mueller-Mach R, Mueller G, Schnick W (2007) Proc SPIE-Int Soc Opt Eng 6669:66690P/1
98. Stadler F, Oeckler O, Senker J, Hőppe HA, Kroll P, Schnick W (2005) Angew Chem Int Ed 44:567
99. van Krevel JWH, van Rutten JWT, Mandal H, Hintzen HT, Metselaar R (2002) J Solid State Chem 165:19
100. Xie RJ, Hirosaki N, Mitomo M, Suehiro T, Xu X, Tanaka H (2005) J Am Ceram Soc 88(10):2883
101. Grins J, Shen Z, Nygren M, Ekström T (1995) J Mater Chem 5:2001
102. Takahashi K, Hirosaki N, Xie RJ, Harada M, Yoshimura K, Tomomura Y (2007) Appl Phys Lett 91:091923
103. Li YQ, Hirosaki N, Xie RJ, Takeda T, Mitomo M (2008) Chem Mater 20(21):6704
104. Li YQ, de With G, Hintzen HT (2006) J Lumin 116:107
105. Kück S (2001) Appl Phys B 72:515
106. Xie RJ, Hirosaki N, Mitomo M et al (2005) J Phys Chem B 109:9490